

## **Molecular Spectroscopic Study on Interaction between Eugenol and Hesperidin Nanoparticles**

**S.Bakkialakshmi<sup>\*1</sup>, S.Pushpa<sup>2</sup>**

<sup>1,2</sup>Department of Physics, Annamalai university, Annamalainagar,  
Tamilnadu, India

### **Abstract**

Parkinson's disease is characterised by a progressive loss of dopaminergic neuron in the substantia nigra. Hesperidin is a free radical scavenger that has been shown to have a protective effect against oxidative insults. An antioxidant can neutralise the free radical by accepting or donating an electron to eliminate the unpaired condition. Ionic gelation with tripolyphosphate and chitosan was used to render hesperidin-loaded chitosan nanosuspension. UV-Visible, FTIR, SEM, XRD, and a particle size analyser were used to classify hesperidin nanoparticles. Eugenol association with hesperidin nanoparticles was investigated using spectroscopic methods such as UV-Visible, Fluorescence, Synchronous fluorescence, lifetime measurements, FRET and antibacterial activity. Eugenol–Hesperidin nanoparticles were found to have a complex formation. The distance between the donor and the acceptor was determined using Forster's non-radiation energy transfer principle. Antibacterial behaviour was investigated as well.

**Keywords:** Hesperidin nanoparticles, Eugenol, Spectroscopy techniques, Fluorescence quenching.

### **Introduction**

Parkinson's disease is more common in people over the age of 65, and it's linked to genetics, toxins, oxidative stress, mitochondrial defects, free radicals, and alpha-synuclein aggregation, which is thought to be the primary cause of Parkinson's disease. Following Alzheimer's disease, it is the second most common neurodegenerative extrapyramidal motor disorder. Antioxidants can remove the unpaired state by accepting or donating an electron to neutralise the free radical. [1-5]. Flavonoids like hesperidin have been shown to protect against neurodegenerative disease by acting as antioxidants.[6]. The antioxidative activity of hesperidin is based on the number and order of OH groups, as well as the existence of a C4'-C8' double bond conjugated seeking 4-keto group in the flavonoid structure. It also has anti-inflammatory, antiviral, anticancer, sedative, Huntington's stroke, and Alzheimer's potential. Medicinal aromatic plants have a variety of health and well-being-promoting properties[7, 8]. Antioxidant, digestion-stimulating, hypolipidemic, anti-inflammatory, and anti-carcinogenic essential oils from these plants [7,8]. Essential oils high anti-oxidant potential is attributed to phenolic and polyphenolic compounds, which are used as preservatives in the food industry [9]. Cloves main flavour chemical, eugenol (4-allyl-2-methoxyphenol), is commonly used as an ingredient in foods, cosmetics, and aromatherapy products, as well as in a number of industrial products [7-9]. It's used to make isoeugenol, which is used to make vanillin, which is an artificial vanilla substitute [9]. It's useful in the production of plastics and rubbers because it's an antioxidant [7–9]. Due to the formation of phenoxy radicals and then quinone intermediates, eugenol acts as a powerful oxidant at higher concentrations, triggering increased generation of tissue-damaging free radicals, causing inflammatory and allergic reactions[10, 11]. As a result, the current research is being carried out in order to better understand the relationship between Eugenol and Hesperidin nanoparticles.

## **2. Materials and methods**

Eugenol and hesperidin were purchased from Sigma–Aldrich, Bangalore. Low molecular weight Chitosan(CS) and sodium tripolyphosphate were purchased from Sisco research laboratory, Chennai.

### **2.1 Preparation of Hesperidin Nanosuspension and Optimization of Preparation Process**

Nanosuspension with relevant stabilizer was prepared by ionic gelation method. Chitosan solution (0.1% w/v) was prepared by dissolving chitosan in 100 ml of 1% v/v of acetic acid, and the resulting solution was stirred at 1500 rpm for 30 min on magnetic stirrer. TPP solution of 0.1% was prepared by dissolving 100 mg of TPP in 100 ml of deionized water. 100 mg of hesperidin was added to TPP solution and mix to form a homogenous mixture by stirring with a glass rod. Add the above mixture of TPP and hesperidin solution drop by drop (10 ml) to the chitosan solution and kept stirring at 2,500 rpm for 3h on stirrer. Nanoparticles were obtained on the addition of a TPP and hesperidin solution to a chitosan solution. The nanoparticle suspension is then centrifuged at 15,000 rpm for 10 min using high-speed centrifuge. Discard the sediment and preserve the supernatant. The formation of nanoparticles results in interaction between the negative groups of TPP and the positively charged amino groups of chitosan.

## **2.2 Characterization of Hesperidin -Loaded Chitosan Nanoparticles**

### **2.2.1 Particle Size**

The size of the prepared nanoparticles was analyzed using MICROMRTICS CPE-11 Nano plus

### **2.2.2 Fourier-transform infrared (FTIR) study**

FTIR analysis of pure hesperidin mixture (hesperidin, chitosan, and TPP) was performed, and the spectrum was obtained using FT-IR (IR spectrometer Cary-630 FTIR Agilent Technology). All spectra were recorded within a range of 4000–500  $\text{cm}^{-1}$ .

### **2.2.3 SEM analysis**

Joel Sem Model, Jsm –IT 200 Scanning Electron Microscope was used to record the SEM photographs of hesperidin Nanoparticles.

### **2.2.4 XRD**

The XRD for H-NP analyzed by X-Ray Diffractometer (BRUCKER D8 Advance).

## **2.3 Methods**

### **2.3.1. UV/Vis absorption experiments**

The absorption spectra of Eugenol and in different concentrations of hesperidin nanoparticles have been recorded using SHIMADZU 1800 PC UV/Visible Spectrophotometer

### **2.3.2. Fluorescence steady – state measurements**

The steady – state fluorescence quenching measurements were carried out in a Shimadzu RF 5301 PC Spectrofluorophotometer. The excitation wavelength was 280 nm. The emission wavelength was monitored at 317nm. The excitation and emission slit widths (5nm) and scan rate (200 nm/s) were constantly maintained for all the experiments.

### **2.3.3. Fluorescence lifetime measurement**

Fluorescence lifetime measurements were carried out in a Hariba – Jobin Yvon [spex-sf 13-11] Spectrofluorimeter. The interchangeable nano LED (280 nm) was used as excitation source. The fluorescence decay of Eugenol was measured with a monochromator – Photo multiplier setup. The data points were fitted by mono exponential decay functions.

### **2.3.4 Antibacterial Activity**

The samples (0.5g) were dissolved in 1ml DMSO. The antimicrobial activity screening was performed with the Muller Hinton agar (MHA) medium for antibacterial activity in the agar well diffusion method. The fungal and

bacterial inocula have been prepared on the nutrient broth medium from 24-hour colonies. The inoculum with McFarland density had been adjusted to obtain a final bacterial density of around  $10^4$  and  $10^6$  CFU/mL. In Whatmann AA filter paper, 50 $\mu$ g each extract was imbibed and applied to the test media previously inoculated with each test strain. Plates for bacteria have been incubated at 37 °C. Zones of inhibition were measured after 24 hours of incubation (12).

### 3. Results and Discussion

#### 3.1 Characterization of Hesperidin nanoparticles

UV, FTIR, Scanning electron microscope (SEM), XRD, and particle size analyser were used to characterise the formed chitosan nanoparticles.

##### (i) UV – Visible Spectroscopy

The primary method for determining the size and shape of nanoparticles is ultraviolet spectrometry. Since colloids have a high absorption peak due to surface Plasmon excitation, it is very sensitive to the presence of colloids. SHIMADZU 1800 PC UV/Visible Spectrophotometer was used for UV-Visible Spectral Analysis. A small aliquot of the reaction mixture was taken and a spectrum was taken at wavelengths ranging from 200 to 800 nm. As shown in Fig.1, the UV-Visible results show a typical absorption peak of quercetin at 283 nm.

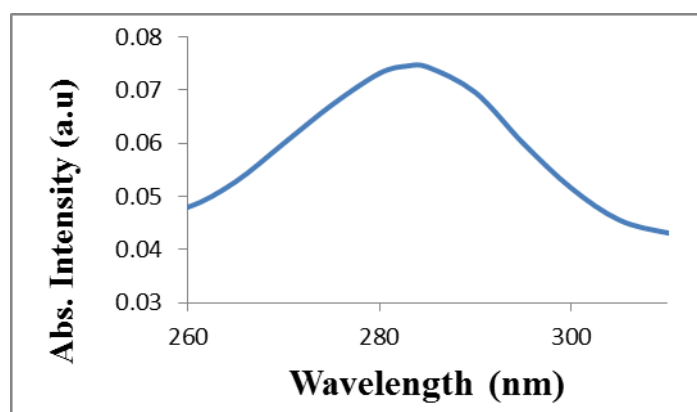


**Fig 1: UV/Vis absorption spectra of Hesperidin nanoparticles**

##### (ii) Fourier Transform Infrared Spectroscopy (FTIR)

Many organic chemicals, polymers, paints, coatings, adhesives, lubricants, semiconductor materials, coolants, gauges, biological samples, inorganics, and minerals use FTIR to study their chemical composition. FTIR [12] can be used to analyse a range of materials, including bulk materials, films, liquids, solids, pastes, powders, fibres, and other materials. The FTIR spectra revealed information about the local molecular environment of organic molecules on nanoparticle surfaces. FTIR analysis may be used for quantitative (amount) analysis as well as qualitative (identification) analysis of materials when appropriate criteria are used. The extreme absorption peaks of quercetin nanoparticles (Table1) corresponded to O-H Stretching of the alcohol group at 3329. The C-H Stretching of the alkane group can be seen in the band absorbed at 2918.

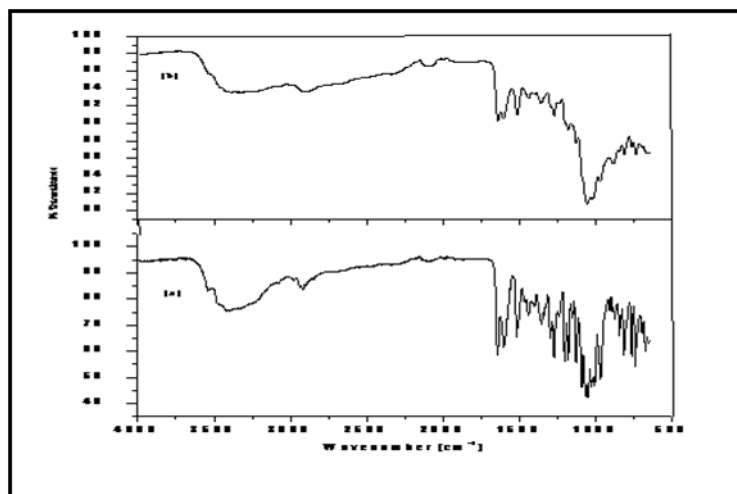


**Fig.2: FTIR spectra of a) Hesperidin b) Hesperidin nanoparticles**

The O-H hydroxyl bond was represented by the absorption band at 2398. The other absorption peak at 1110 was due to C-O stretching of the ether group, as shown in Fig.2.

### (iii) Scanning Electron Microscopy

The surface morphologies of the nanoparticles were evaluated using SEM. SEM images were collected at various magnifications. A thin specimen is scanned with a fine, highly concentrated beam of electrons, and the electrons that pass through the thin sample are captured on a detector mounted underneath the sample, resulting in the desired bright - field images. The SEM image (Fig.3) revealed a nanoparticle with a spherical shape. The transmitted electrons are directed onto a conventional detector through an electron multiplier, which is a gold layer.

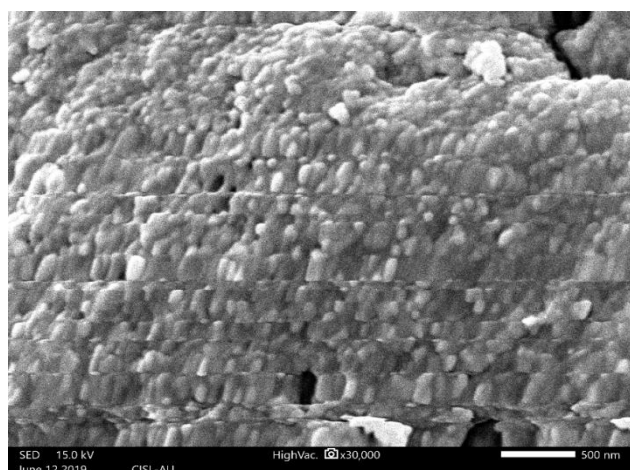


**Fig.3: SEM image of Hesperidin nanoparticles**

### (iv) XRD Analysis

An x-ray diffractometer was used to determine the crystalline state of the samples. The Hesperidin XRD Patterns at flow rates of 8 and 10 ml/min, as well as the sample, revealed the existence of numerous distinct peaks at  $2\theta$  (39.82°). As the findings are expressed in, this indicated that the drug was of a high crystalline nature (Fig.4)

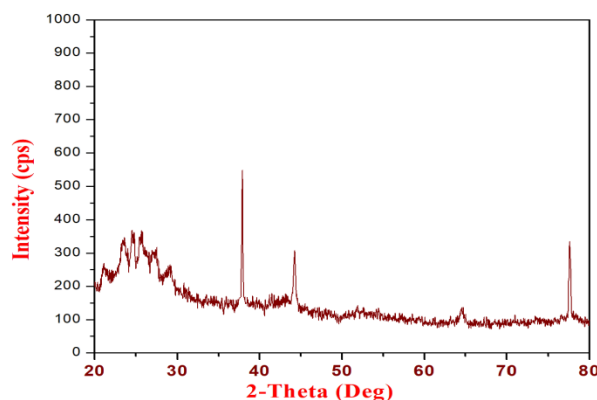


Fig.4: XRD spectra of Hesperidin nanoparticles

(v) Particle size analyser

A particle size analyzer was used to determine the particle size. The experiment was carried out at a temperature of 250°C with water as the solvent. According to the findings, the hesperidin formulation has an average particle size of 256.9 nm (Fig.5). As anticipated, the obtained particles have a nanometer size range. Nanoparticle colloid has a variety of advantageous properties, including the ability to sedimentate slowly due to its nano-size. The polydispersibility index obtained from particle size measurement was 0.384.

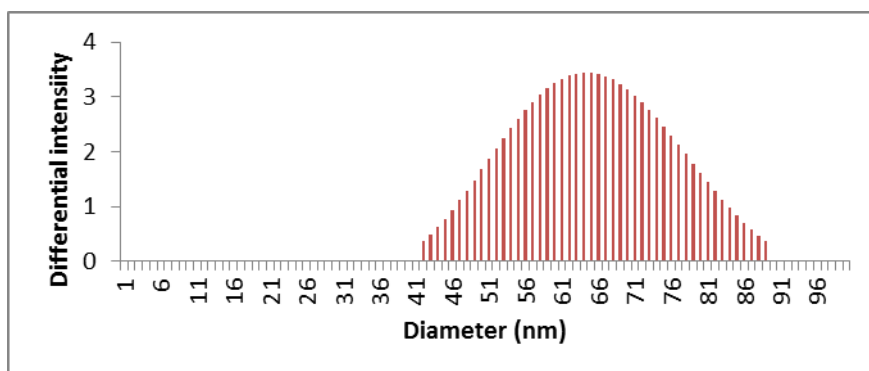
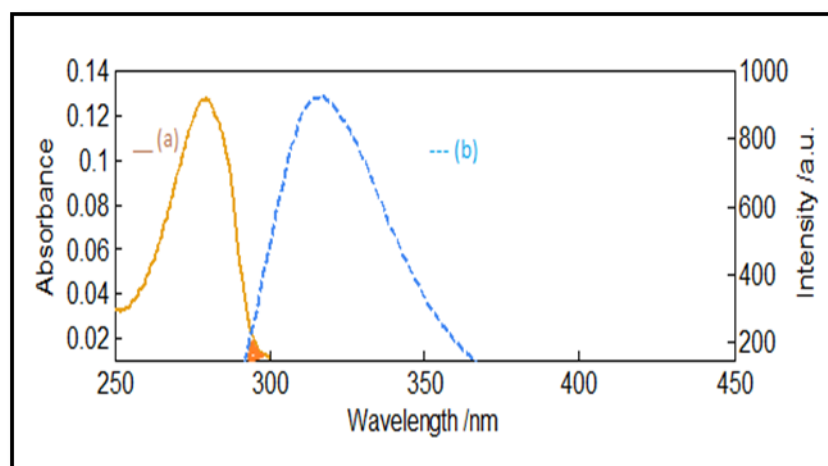


Fig .5: Particle size analyser of Hesperidin Nanoparticles

The polydispersibility index defines the distribution of particle sizes present in the preparation of nanoparticles; the lower the number, the more uniform the particle sizes; if there is a substantial size difference between the larger and smaller particles, it will affect the particles' characteristics.

### 3.2 Absorption characteristics of Eugenol with hesperidin nanoparticles

Eugenol absorption and emission spectra are depicted in Figure 6. It has a maximum absorption wavelength of 280 nm and a maximum emission wavelength of 317 nm. Initially, the ground state interaction between eugenol and quenchers molecules must be measured before the quenching experiments can be completed.



**Fig.6: Absorption (a) and Emission spectra (b) of Eugenol.**

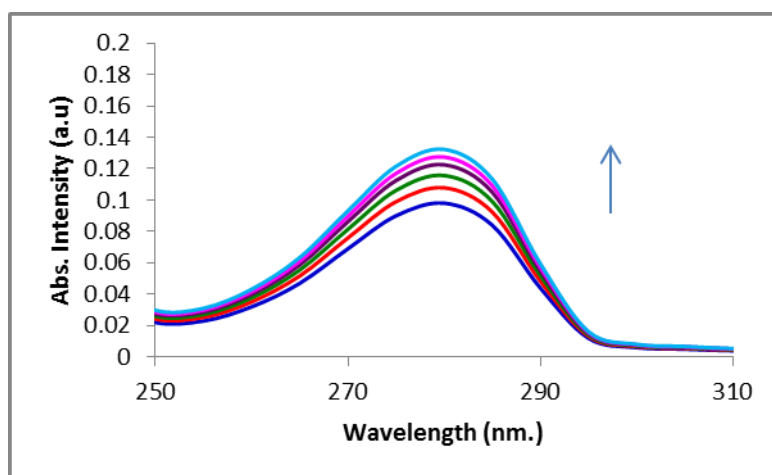


**Fig .7: UV/Vis absorption spectra of Eugenol with different concentrations of Hesperidin nanoparticles (mol L<sup>-1</sup>) (1)0, (2)0.2, (3)0.4, (4) 0.6, (5) 0.8, (6) 1.0.**

The absorption spectra of a mixture of eugenol and hesperidin nanoparticles were used to confirm the formation of the ground state complex. Figure 7 indicates the absorption spectrum of Eugenol in the presence and absence of hesperidin nanoparticles. The absorption of eugenol is increased when hesperidin nanoparticles are added. This demonstrates that eugenol can form a ground state complex with hesperidin nanoparticles.

### 3.3 Fluorescence quenching of eugenol by Hesperidin nanoparticles.

The hesperidin nanoparticles effectively quenched the fluorescence emission of eugenol, and the emission quenching measured by the steady state method is shown in Fig 8. The stern-Volmer Equation was used to measure the bimolecular quenching rate constants ( $k_q$ ).

$$I_0/I = 1 + K_{SV} [Q] = 1 + K_q \tau_0 [Q] \quad (1)$$

Where  $I_0$  is the fluorescence Intensity of the fluorophore in the absence of the quencher,  $I$  is the fluorescence intensity of the fluorophore in the presence of quencher,  $k_{sv}$  is the stern – volmer constant,  $\tau_0$  is the fluorescence lifetime in the absence of quencher,  $[Q]$  is the concentration of the quencher and  $K_q$  is the bimolecular quenching rate constant

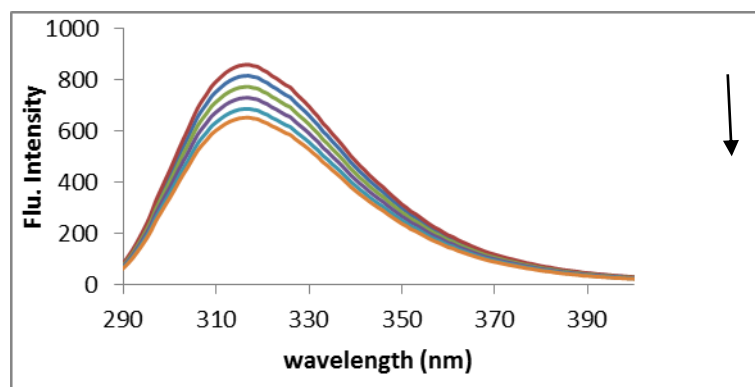


**Fig.8: Steady–State fluorescence spectra of Eugenol with different concentrations of Hesperidin nanoparticles (mol L<sup>-1</sup>) (1) 0, (2) 0.2, (3) 0.4, (4) 0.6, (5) 0.8, (6) 1.0**

Figure 8 depicts the effect of rising hesperidin nanoparticle concentration on eugenol fluorescence emission. The addition of hesperidin nanoparticles to a eugenol solution caused the fluorescence emission to be quenched, but no peak change or new peak was observed. A linear plot of (Fig .9)  $I_0/I$  against  $[Q]$  has been drawn according to eqn (1).  $K_{sv}$  values have been determined based on the slope.

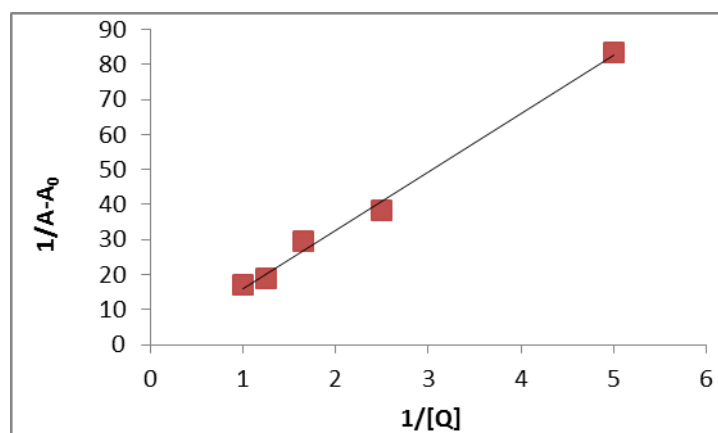


**Fig.9: Plot of  $\left[ \frac{1}{A-A_0} \right]$  versus  $\left[ \frac{1}{[Q]} \right]$  for EG**

Table 2 compiles the bimolecular quenching rate constant ( $k_q$ ) and the corresponding electrochemical results. The number of hydroxyl groups bound to the aromatic ring and their structure, as well as the position of the aromatic -OH ring, are all related to the ability of flavonoids compounds to scavenge free radicals (13,14)

**Table 2: Stern – Volmer ( $K_{sv}$ ) and bimolecular quenching rate constant ( $K_q$ ) of Eugenol with Hesperidin nanoparticles**

Quencher	$K_{sv} \times 10^5$ (L mol <sup>-1</sup> )	$K_q$ (L mol <sup>1</sup> S <sup>-1</sup> )	R <sup>a</sup>	S.D <sup>b</sup>
Hesperidin nanoparticles	0.21	2.39	0.9	0.44

### 3.4 Fluorescence lifetime measurements of Eugenol with Hesperidin nanoparticles

Fluorescence lifetime calculation is a powerful method for evaluating the form of interaction that exists between the donor and acceptor systems. The most precise approach for distinguishing between static and dynamic quenching is to calculate fluorescence lifetime [15].

Though the decay traces of eugenol were plotted in the absence and presence of hesperidin nanoparticles in Fig 10, the lifetime of eugenol is the same in both cases, so no merging of the kinetic traces was observed (the plots looks not like a single decay curve). This shows that the quenching of eugenol was static in nature. As a result, static quenching occurs, and no new lifetime formation occurs. Since static quenching is caused by the creation of a complex between the fluorophore and the quencher, the binding constant ( $k$ ) has been determined. As a result, the binding constant ( $k$ ) was calculated using the method described within following section.

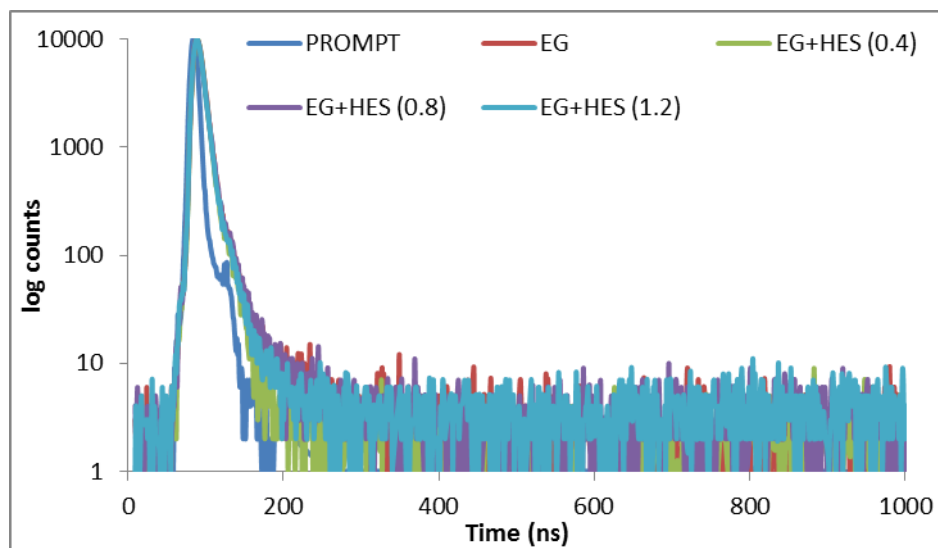


**Fig.10: Time-resolved fluorescence spectra of Eugenol (EG) with different concentrations of Hesperidin Nanoparticles ( $\text{mol dm}^{-5}$ ) (1)0, (2) 0.4, (3) 0.8, (4) 1.2**

**Table 3: Fluorescence life time and Relative amplitudes of Eugenol with different concentrations of Hesperidin Nanoparticle**

Concentration (M)	Lifetime (ns)		Average life time $\times 10^{-9}$ sec	Relative amplitude		$\chi^2$	S.D $10^{-11}$ sec	
	$\tau_1$	$\tau_2$		B <sub>1</sub>	B <sub>2</sub>		$\tau_1$	$\tau_2$
EG	6.67	5.23	0.7458	98.28	1.72	1.089	4.17	3.26
EG +H NP (0.4)	6.32	3.50	0.7329	96.49	3.51	1.182	4.14	1.44
EG +H NP(0.8)	3.50	6.43	0.6912	98.32	1.68	1.209	2.99	3.83
EG +H NP (1.2)	6.26	2.16	0.6471	98.63	1.37	0.815	9.50	2.33

### 3.5 Binding constant and number of binding sites

Large  $k_q$  values above the diffusion-controlled limit suggest that the fluorophore and quencher have a binding interaction [12]. The binding constant formula[13] can be used to explain the relationship between the strength



and the concentration of quencher in static quenching. The following equation can be used to determine the relationship between fluorescence intensity and quencher medium.



B is the fluorophore, Q is the quencher, and  $Q_n \dots B$  is the postulated complex between a fluorophore and n molecules of the quencher. The constant K is given by

$$K = [Q_n \dots B] / [Q]^n [B] \quad (3)$$

If the total amount of biomolecules (bound or unbound with the quencher) is  $B_0$ , then  $[B_0] = [Q_n \dots B] + [B]$ , where [B] is the concentration of unbound biomolecules, then the relationship between fluorescence strength and the unbound biomolecules is  $[B]/[B_0] = F/F_0$ .

$$\log [F_0 - F/F] = \log K + n \log [Q] \quad (4)$$

where K is the binding constant and n is the number of binding sites.

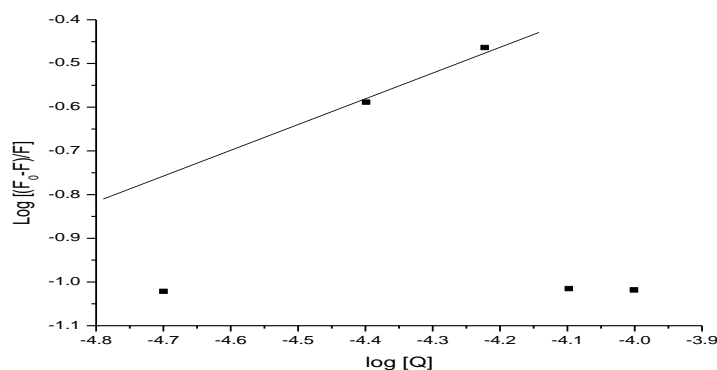


**Fig.11: Double log plot of EG with Hesperidin Nanoparticles**

As seen in the figures, the value of K was calculated from the intercept of  $\log[(F_0-F)/F]$  versus  $\log[Q]$ . Tables 2 and fig.11 show the of binding constant (k) and number of binding sites (n) for all antioxidants. .

. . All of the curves had a correlation coefficient greater than 0.980, suggesting that the relationship between eugenol and antioxidants fits the site binding model underlying Eq (4).

### 3.6 Energy transfer between Eugenol and Hesperidin nanoparticles.

In addition to radiation and reabsorption, the Förster theory of molecular resonance energy transfer suggests that a transfer of energy could occur by direct electrostatics interaction between the primarily excited molecule and its neighbours [14]. Eq.(5) may be used to measure the distance r of binding between eugenol and hesperidin, according to theory [15].

$$E = 1 - \left( \frac{F}{F_0} \right) = \frac{R_0^6}{(R_0^6 + r^6)} \quad (5)$$

where r denotes the binding distance between the donor and the receptor, and  $R_0$  denotes the critical distance when the transfer efficiency is 50%. E is the efficiency of energy transfer. The equation is used to determine the value of  $R_0$ .

$$R_0^6 = 8.8 \times 10^{-25} k^2 n^4 \phi J \quad (6)$$

In Eq. (6),  $K^2$  is orientation factor,  $n$  is the refractive index of the medium,  $\phi$  is the fluorescence quantum yield of the donor,  $J$  is the spectral overlap effect between the donor's emission spectrum and the acceptor's absorption spectrum, which can be determined using the following equation:

$$J = \frac{\int_0^\alpha F(\lambda) \Sigma(\lambda) \lambda^4 \Delta\lambda}{\int_0^\alpha F(\lambda) \Delta\lambda} \quad (7)$$

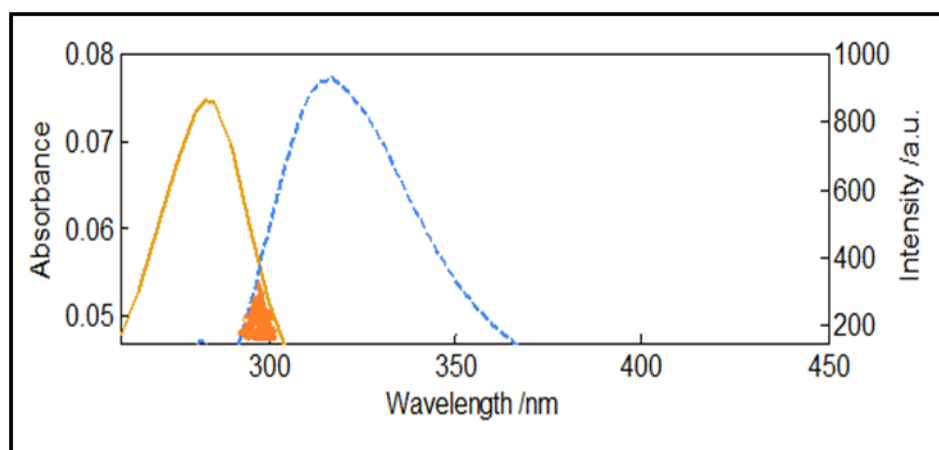


**Fig.12: The overlap of UV absorption spectra of Hesperidin- NP (solid line) with the fluorescence emission spectra of Eugenol (dotted line)**

where  $F(\lambda)$  is the fluorescence reagent fluorescence intensity. When the wavelength is  $k$ ,  $e(k)$  is the acceptor molar absorbance coefficient at that wavelength.  $J$ ,  $E$ , and  $R_0$  can be determined using these relationships, and the value  $r$  can be calculated as well. The fluorescence spectra of Eugenol and the absorption spectra of hesperidin nanoparticles are shown in Figure 12. The fluorescence spectra of Eugenol and the absorption spectra of hesperidin nanoparticles are shown in Figure 12. The data are presented in table 4. The donor to acceptor distance ( $r$ ) is less than  $8\text{nm}$ (16), which meets the requirements for energy transfer, implying that energy transfer between Eugenol and hesperidin nanoparticles is highly likely.

**Table 4: Efficiency transfer energy (E) and Critical energy transfer distance ( $R_0$ ) of EG with Hesperidin nanoparticles**

Quencher	Energy(E) (eV)	$R_0$ (nm)	J ( $\text{cm}^{-3}\text{M}^{-1}$ )( $10^{16}$ )	r (nm)
Hesperidin nanoparticles	0.74	1.8	4.01	1.5

### 3.7 Synchronous fluorescence

Synchronous fluorescence spectra may provide details about the molecular microenvironment around the fluorophore by scanning the excitation and emission monochromators at the same time while maintaining a constant wavelength interval ( $\Delta\lambda$ ). When  $\lambda$  is fixed at 60 and 30 nm, synchronous fluorescence indicates characteristic information about the complexes [17]. Figures 13 ( $\Delta\lambda = 60 \text{ nm}$ ) and 13 ( $\Delta\lambda = 30 \text{ nm}$ ) show the effects of flavonoid on the synchronous fluorescence spectra of eugenol.

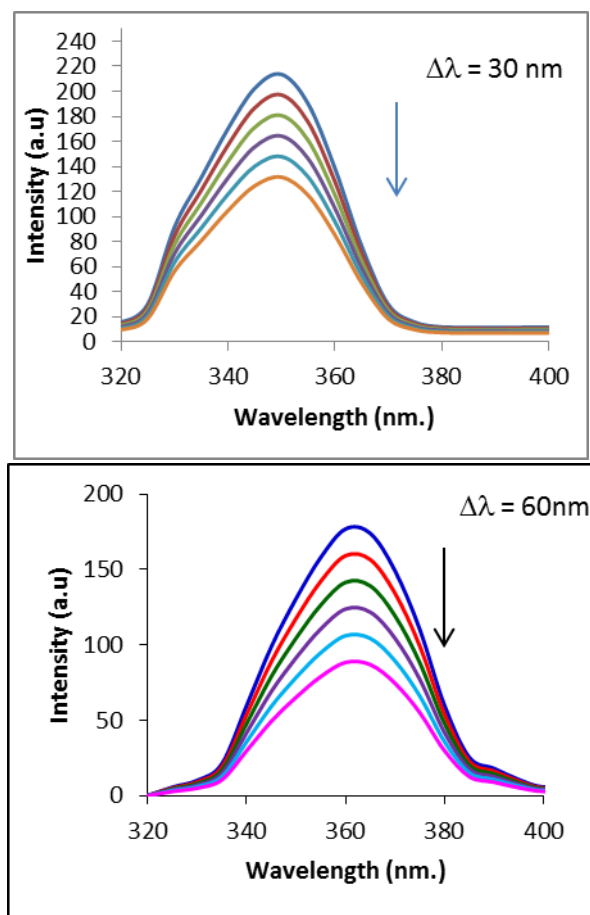


Fig.13: Synchronous Fluorescence Spectra for EG with Hesperidin having  $\Delta\lambda = 30 \text{ nm}$  and  $\Delta\lambda = 60 \text{ nm}$

### 3.8 Antibacterial Activity

Because the terpene components of essential oils disrupt the bacterial membrane, essential oils exhibit antibacterial activity (17). The agar well diffusion method was used to test the antibacterial activity of quercetin nanoparticles–Eugenol. ( Fig 14) .

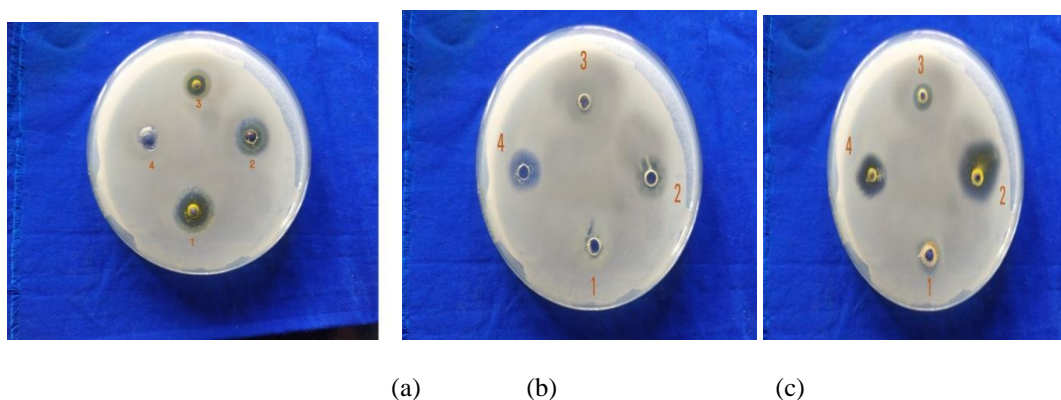


Fig 14: The antibacterial activity of (a) Eugenol (b) Hesperidin nanoparticles (c) Eugenol+Hesperidin nanoparticles (1. staphylococcus sp., 2. E.Coli, 3. V.B, 4. Salmonella sp.)

As evidenced by the plates, the sample exhibited strong antibacterial activity. Eugenol hesperidin nanoparticles, in short, are effective Gram-negative and Gram-positive antibacterial materials.

#### **4 . Conclusion**

UV, FTIR, SEM, XRD, and particle size analyzers were used to create and characterise hesperidin nanoparticles. The fluorescence, Eugenol, is quenched by hesperidin nanoparticles. The constant of quenching rate has been determined. The binding constant and binding site have been determined. The distance between the donor and the acceptor has been determined. FRET was used to calculate the distance between the donor and acceptor. This study also discovered that these nanoparticles have antibacterial activity against both Gram positive and Gram negative bacteria, indicating that they should be investigated further for antimicrobial applications.

#### **REFERENCES**

1. Lü, J. M., Lin, P. H., Yao, Q., & Chen, C. (2010). Chemical and molecular mechanisms of antioxidants: experimental approaches and model systems. *Journal of cellular and molecular medicine*, 14(4), 840-860.
2. Faraci, F. M., & Heistad, D. D. (1998). Regulation of the cerebral circulation: role of endothelium and potassium channels. *Physiological reviews*, 78(1), 53-97.
3. Lum, H., & Roebuck, K. A. (2001). Oxidant stress and endothelial cell dysfunction. *American Journal of Physiology-Cell Physiology*, 280(4), C719-C741.
4. Balaban, R. S., Nemoto, S., & Finkel, T. (2005). Mitochondria, oxidants, and aging. *cell*, 120(4), 483-495.
5. Beckman, K. B., & Ames, B. N. (1998). The free radical theory of aging matures. *Physiological reviews*.
6. Tamilselvam, K., Nataraj, J., Janakiraman, U., Manivasagam, T., & Essa, M. M. (2013). Antioxidant and anti-inflammatory potential of hesperidin against 1-methyl-4-phenyl-1, 2, 3, 6-tetrahydropyridine-induced experimental Parkinson's disease in mice. *International Journal of Nutrition, Pharmacology, Neurological Diseases*, 3(3), 294.
7. Son, K. H., Kwon, S. Y., Kim, H. P., Chang, H. W., & Kang, S. S. (1998). Constituents from *Syzygium aromaticum* Merr. et Perry. *Natural Product Sciences*, 4(4), 263-267.
8. Wang, H. F., Wang, Y. K., & Yih, K. H. (2008). DPPH free-radical scavenging ability, total phenolic content, and chemical composition analysis of forty-five kinds of essential oils. *Journal of cosmetic science*, 59(6), 509-522.
9. Backheet, E. Y. (1998). Micro determination of eugenol, thymol and vanillin in volatile oils and plants. *Phytochemical Analysis: An International Journal of Plant Chemical and Biochemical Techniques*, 9(3), 134-140.
10. Nam, H., & Kim, M. M. (2013). Eugenol with antioxidant activity inhibits MMP-9 related to metastasis in human fibrosarcoma cells. *Food and chemical toxicology*, 55, 106-112.
11. Southwell, I. A., Russell, M. F., & Davies, N. W. (2011). Detecting traces of methyl eugenol in essential oils: tea tree oil, a case study. *Flavour and fragrance journal*, 26(5), 336-340.
12. Papadopoulou, A., Green, R. J., & Frazier, R. A. (2005). Interaction of flavonoids with bovine serum albumin: a fluorescence quenching study. *Journal of agricultural and food chemistry*, 53(1), 158-163.

13. Duthie, G. G., Duthie, S. J., & Kyle, J. A. (2000). Plant polyphenols in cancer and heart disease: implications as nutritional antioxidants. *Nutrition research reviews*, 13(1), 79-106.
14. Wilmsen, P. K., Spada, D. S., & Salvador, M. (2005). Antioxidant activity of the flavonoid hesperidin in chemical and biological systems. *Journal of agricultural and food chemistry*, 53(12), 4757-4761.
15. Nijveldt, R. J., Van Nood, E. L. S., Van Hoorn, D. E., Boelens, P. G., Van Norren, K., & Van Leeuwen, P. A. (2001). Flavonoids: a review of probable mechanisms of action and potential applications. *The American journal of clinical nutrition*, 74(4), 418-425.
16. Jung, H. A., Jung, M. J., Kim, J. Y., Chung, H. Y., & Choi, J. S. (2003). Inhibitory activity of flavonoids from *Prunus davidiana* and other flavonoids on total ROS and hydroxyl radical generation. *Archives of pharmacal research*, 26(10), 809-815.
17. Lombard, K. A., Geoffriau, E., & Peffley, E. (2002). Flavonoid quantification in onion by spectrophotometric and high performance liquid chromatography analysis. *HortScience*, 37(4), 682-685.